Detection of dynamical structure from short and noisy chaotic series

Chao Tao,[1,2,*] Xiaojun Liu,[1] and Gonghuan Du[1]
[1]*Key Laboratory of Modern Acoustics, Ministry of Education, Nanjing University, Nanjing 210093, People's Republic of China*
[2]*Department of Surgery, Division of Otolaryngology Head and Neck Surgery, University of Wisconsin Medical School, Madison, Wisconsin 53792-7375, USA*

(Received 18 August 2009; revised manuscript received 2 February 2010; published 20 April 2010)

A method is proposed to detect the dynamical structure hiding behind complex chaotic series by comparing prediction performance of trial functions. This method is valid even when the original system is contaminated with noise or only a relatively short data series is recorded. Using this method, the dynamical structure of the Gray-Scott model is detected from its rich spatiotemporal patterns. Finally, this method is successfully applied to the experimental data of Chua's circuit, which promises its potential of the application to realistic systems.

DOI: 10.1103/PhysRevE.81.046209 PACS number(s): 05.45.Gg, 05.45.Tp

I. INTRODUCTION

Many complex natural or artificial phenomena are often governed by simple nonlinear laws [1]. Direct observation of the intrinsic mechanism governing these phenomena cannot be achieved in experiments. The time series of these systems can usually be recorded experimentally. Therefore, reconstructing the dynamical system (mathematic equations and their parameters) from the measured complex superficies has been an important topic of nonlinear science [2–12]. However, because of the properties of chaos, such as the irregular behavior, ergodicity, and the sensitive dependence on initial conditions and parameters, modeling chaos is often difficult. Many previous studies focused on extracting the system parameters by using a so-called standard function or assuming the dynamical structure is known [8–13]. Although, a standard function with numerous functional bases and appropriate parameters could well approach the dynamical properties of the original dynamical system. Most terms of the standard function are actually not the intrinsic structure belonging to the original system. These superfluous terms not only significantly decrease the model performance [7,14], but also prevent researchers from gaining an insight into the dynamical laws behind the complex chaotic phenomena. Therefore, the detection of the intrinsic structure is of significance for improving the global modeling. Moreover, the intrinsic structure itself contains important information of the original system.

Some works have been done to select the model structure [10,15–22] by using various methods such as zeroing-and-refitting [15], the model entropy [16], the maximum description length [17,18], proper orthogonal decomposition and error reduction ratio [19,20], minimum description length principle [22], or taking into account the prior knowledge [10] of nonlinear systems. However, when the chaotic data series is too short or contains noise, these methods are often ineffective, which limit their application in practice. To the best of our knowledge, this problem has not been well resolved.

The one-step prediction can reflect the dynamical characteristics of a short and noisy data series [23,24]. Barahona and Poon found that a nonlinear polynomial can provide a much better one-step prediction of chaotic series than a linear polynomial [24]. This is because the nonlinear polynomial has the nonlinear terms of the original chaotic system that the linear one lacks. Based on this finding, they proposed a scheme to detect nonlinear dynamics from a short, noisy time series by comparing the linear/nonlinear one-step prediction error [24–26].

In this study, we generalize this concept: For any two trial functions (TF) $\Phi_1(x)$ and $\Phi_2(x)$, if one TF can provide a much better one-step ahead prediction of a data series than another, the better one must have some intrinsic structures of the original system, which are not taken in by another TF, i.e., the structure discrepancy between the two TF contains some intrinsic structures of the original system. Based on this concept, we develop a scheme to recover the system structure from a complex chaotic pattern.

In the following discussion, "intrinsic structure" means the detected structure, which really belongs to the original system; "superfluous structure" indicates the selected structure that actually does not exist in the original system; "missed structure" implies the structure that does not be detected but really belongs to the original system.

II. METHOD

Without loss of generality, let us consider the k-th variable x_k of the nonlinear system $\mathbf{x}(t+1)=\mathbf{f}[\mathbf{x}(t),\mathbf{x}(t-1),\ldots,\mathbf{x}(t-M)]$ with $\mathbf{x}(t)=[x_1(t),x_2(t),\ldots,x_k(t),\ldots,x_K(t)]^{\mathrm{T}}$,

$$x_k(t+1)=f_k(x_1(t),\ldots,x_1(t-M),x_2(t),\ldots,x_2(t-M),x_3(t),\ldots,x_K(t-M))+s(t), \quad (1)$$

where K is the number of variables and M is the memory of the system. $s(t)$ is a stochastic noise. In order to focus on the structure detection, we assume that the vector $\mathbf{x}(t)$ has been directly measured or reconstructed by using the methods of time delay [27] or sequential derivatives [7–9]. A I-term TF is constructed to approach the original system [Eq. (1)],

*Author to whom correspondence should be addressed; taochao@nju.edu.cn

$$y_k(t+1) = \sum_{i=1}^{I} c_i \phi_i(y_1(t), \ldots, y_1(t-M), y_2(t), \ldots, y_2(t-M), y_3(t), \ldots, y_K(t-M)), \quad (2)$$

where ϕ_i and c_i are the functional bases and their coefficients. Anyway, if the TF takes in numerous bases, it could include all possibility of the original system's structures. However, only a few of these bases really belong to the original system. Our purpose is to detect these intrinsic structures.

We define a truncated TF constructed with the first r-term of the whole TF [Eq. (2)] as r-term TF. Substituting $\mathbf{x}(t) \equiv \mathbf{y}(t)$ into this truncated TF, its coefficient c_i can be estimated using a least-squares method. With the known coefficients c_i, the one-step predicted series can be calculated by $\tilde{x}_k(t+1) = \Sigma_{i=1}^{r} c_i \phi_i[x_1(t), \ldots, x_K(t-M)]$ and the prediction error power is defined as $\varepsilon(r)^2 = \Sigma_{t=1}^{N}[\tilde{x}_k(t) - x_k(t)]^2 / \Sigma_{t=1}^{N}[x_k(t) - \bar{x}_k(t)]^2$, where $\bar{x}_k(t)$ is the time average value of $x_k(t)$ and N is the data length. To quantify the difference of prediction performance between the truncated r-term TF $\Sigma_{i=1}^{r-1} c_i \phi_i + c_i \phi_i$ and $(r-1)$-term TF $\Sigma_{i=1}^{r-1} c_i \phi_i$, we define a parameter "information discrepancy" as

$$V(1) = -1/N,$$

$$V(r) = \log[\varepsilon(r-1)/\varepsilon(r)] - 1/N \quad (r > 1), \quad (3)$$

Clearly, $V(r)$ and the information criterion $C(r) = \log \varepsilon(r) + r/N$ [24] can be linked to each other by $C(r) = -V(1) - V(2) - \ldots - V(r)$. Large $V(r)$ indicates that the structure difference (ϕ_r) between r-term TF and $(r-1)$-term TF is highly related with the original system. An iterative scheme is employed to detect the intrinsic structure of the original system from $V(r)$ and $C(r)$ value.

For the first iterative step, the $V(r)$ value of each basis in the initial TF [Eq. (2)] is calculated. The basis are sorted by the decrease in their $V(r)$ value and a TF is obtained $y_k(t+1) = \Sigma_{i=1}^{I} c_i^{(1)} \phi_i^{(1)}[y_1(t), \ldots, y_K(t-M)]$. It is noticeable that the TF looks similar to the initial TF. However, the sequences of the functional basis in them are different. We add a superscript (1) to indicate this point. For the j-th iterative step, the $V(r)$ value of bases in the TF obtained by the $(j-1)$-th iteration is calculated. Sorting the basis $\phi_i^{(j-1)}$ $(i = j, \ldots, M)$ by the decrease in $V(r)$, the basis with the largest $V(r)$ is moved to the j-th of the TF $y_k(t+1) = \Sigma_{i=1}^{I} c_i^{(j)} \phi_i^{(j)}[y_1(t), \ldots, y_K(t-M)]$. After I-step iteration, the procedure is finished and the final TF can be obtained:

$$y_k(t+1) = \sum_{i=1}^{I} c_i^{(I)} \phi_i^{(I)}[y_1(t), \ldots, y_K(t-M)], \quad (4)$$

$C(r)$ of the final TF is calculated. The first $r_{\min}$ functional bases, which make $C(r_{\min}) \leq C(r)$ for $\forall r \in [1, I]$, are the detected dynamical structure of the original system.

III. NUMERICAL EXAMPLES

To intuitively show how this structure detection scheme works, a chaotic series $x(n)$ is generated by the logistic map $x(n+1) = 3.7x(n)[1 - x(n)] + s(n)$, where $s(n)$ is a white noise with a standard deviation 0.0058. A complex polynomial with degrees 3 and 2 memories $y(n+1) = c_1 + c_2 y(n) + c_3 y(n-1) + c_4 y(n)^2 + c_5 y(n)y(n-1) + c_6 y(n-1)^2 + c_7 y(n)^3 + c_8 y(n)^2 y(n-1) + c_9 y(n)y(n-1)^2 + c_{10} y(n-1)^3$ is used as the initial TF. Most terms [except for $y(n)$, $y(n)^2$] of this TF are superfluous. As shown in Fig. 1, $C(r)$ sharply decrease in $r = 4$, i.e., the term $y(n)^2$ [D in Fig. 1] has the largest $V(r)$. The bases in TF are sorted by the decrease in their corresponding $V(r)$, therefore, the term $y(n)^2$ is moved to the first of the TF. For the second iterative step, the criterion $C(r)$ of the TF is calculated again. The term $y(n)$ [B in Fig. 1] correspond to the largest $V(r)$ of this TF. The second to the tenth terms of this TF are rearranged by the decrease in their $V(r)$ and the term $y(n)$ is moved to the second term. After ten iterations, the final TF is obtained. $C(2)$ is the minimum of $C(r)$ of the final TF and the first two bases $-3.22y(n)^2$ and $3.29y(n)$ (D and B in Fig. 1) are the detected intrinsic structures of the original system.

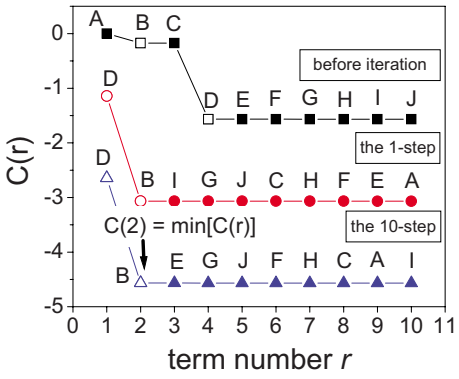

FIG. 1. (Color online). Detecting the intrinsic structure from the chaotic series generated by the logistic map. The information criteria $C(r)$ of the TFs before iteration (square black scatters), after one-step (circle red scatters) and 10-step iteration (triangle blue scatters) are calculated and plotted with the same scale but an offset. The symbols $A, B, C, D, \ldots, J$ represent the TF's ten bases $1, y(n), y(n-1), y(n)^2, \ldots, y(n-1)^3$.

When the chaotic series is generated by a system with multiple memories and high degrees, the intrinsic structure can still be detected from numerous basis candidates. Consider the discrete map with memories $M = 7$ and degrees $D = 3$,

$$\begin{aligned} x(n) = {} & 1 + 0.2x(n-1) + 0.3x(n-3) + 0.1x(n-7) \\ & - 0.6x(n-1)^2 - 0.2x(n-1)x(n-7) - 0.4x(n-4)^2 \\ & - 0.3x(n-2)x(n-5) - 0.1x(n-2)x(n-4)x(n-5) \\ & - 0.1x(n-4)x(n-6)x(n-7) - 0.2x(n-7)^3 + s(n), \end{aligned}$$

where $s(n)$ represents a white noise disturbance. This system has 11 terms and its trajectory evolving in an attractor comprised of fractals in three disconnected domains and visits each of them in a periodic manner [Fig. 2(a) where $s(n) \equiv 0$]. This periodicity was thought to make the nonlinear analysis difficult [24]. A data series with 1000 points generated by this system is used for the structure detection. A TF

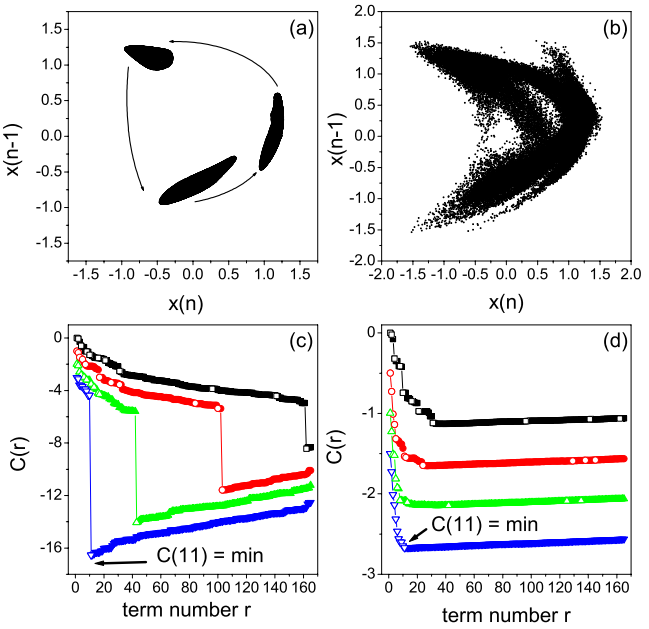

FIG. 2. (Color online). Detecting the intrinsic structure of a discrete map with multiple variables and high degrees. 1000 points are used for the structure detection. (a)–(b) the phase trajectories. (c)–(d) The information criteria $C(r)$ of the initial TF (blue squares), the final TF (downward-pointing blue triangles), and the TFs after one-step (red circles) and two-step iteration (green triangles) are plotted with the same scale but an offset, where the empty scatters represents those intrinsic bases. The left [(a) and (c)] and right [(b) and (d)] columns represent the situations without noise and with noise, respectively.

with numerous bases $y(n)=\Sigma_{i=1}^{I}c_i\phi_i$, where $\phi_i\in\{\Pi_{m=1}^{M}y(n-m)^{d_m}\}$ with $\Sigma_{m=1}^{M}d_m=0,1,\ldots,D$, is used to approach the original system. For $M=8$ and $D=3$, the total term number of this TF is $I=(M+D)!/M!D!=165$. Actually, only 11 elements in this huge basis aggregate are necessary. They are the 1st, 2nd, 4th, 8th, 10th, 16th, 21st, 31st, 96th, 141st, and 162nd bases of the initial TF [the empty scatters in Figs. 2(c) and 2(d)]. The proposed scheme progressively rearranges those intrinsic terms to the front of TF. Finally, $C(11)$ is the minimum of $C(r)$ $(1\le r\le 165)$ and the first 11 terms are just the 11 intrinsic terms belonging to the original system [Fig. 2(c)]. The first 11 bases are 1.00, $-0.2y(n-7)^3$, $0.1y(n-7)$, $-0.1y(n-4)y(n-6)y(n-7)$, $-0.3y(n-2)y(n-5)$, $-0.2y(n-1)y(n-7)$, $-0.1y(n-2)y(n-4)y(n-5)$, $-0.6y(n-1)^2$, $0.3y(n-3)$, $0.2y(n-1)$, and $-0.4y(n-4)^2$ in sequence.

Moreover, even when the system is seriously disturbed by a white noise with a standard deviation 0.0464 [Fig. 2(b)], the proposed detection scheme is still available. As shown in Fig. 2(d), the detected bases are

$$c_1,$$

$$c_{10}y(n-1)^2,$$

$$c_4y(n-3),$$

$$c_{21}y(n-2)y(n-5),$$

$$c_{31}y(n-4)^2,$$

$$c_{162}y(n-7)^3,$$

$$c_{16}y(n-1)y(n-7),$$

$$c_2y(n-1),$$

$$c_{141}y(n-4)y(n-6)y(n-7),$$

$$c_8y(n-7),$$

$$c_{96}y(n-2)y(n-4)y(n-5)$$

($c_1=1.003$, $c_{10}=-0.601$, $c_4=0.303$, $c_{21}=-0.306$, $c_{31}=-0.394$, $c_{162}=-0.199$, $c_{16}=-0.196$, $c_2=0.191$, $c_{141}=-0.102$, $c_8=0.096$, $c_{96}=-0.086$) in sequence.

We have applied the proposed scheme to detecting the continuous equation from complex spatiotemporal pattern governed by partial differential equations (PDEs). The Gray-Scott model [28] has been paid much attention [29] because of its rich spatiotemporal behaviors [1]. The Gray-Scott equations in dimensionless units are

$$\partial u/\partial t = D_u\nabla^2 u - uv^2 + F(1-u), \tag{5}$$

$$\partial v/\partial t = D_v\nabla^2 v + uv^2 - (F+k)V, \tag{6}$$

where $D_u=2.0\times10^{-5}$ and $D_v=1.0\times10^{-5}$ are the dimensionless diffusion coefficients, F is the dimensionless feed rate, and k is the dimensionless rate constant of the second reaction. F and k are control parameters. Equations (5) and (6) with a 200×200 spatial lattice and periodic boundary condition are integrated by using a finite-difference algorithm with mesh space $h=0.01$. The initial homogeneous ($u=1$, $v=0$) status is perturbed by a localized square pulse of size 20×20. After 200 000 steps ($\Delta t=1.0$) integration, the transients die out and the data of 4 000 time steps is used for the detection.

Assuming that the system outputs around the pattern center ($x=0$, $y=0$) [$y_1(t)=u(x,y,t)$, $y_2(t)=u(x,y-h,t)$, $y_3(t)=u(x-h,y,t)$, $y_4(t)=u(x,y+h,t)$, $y_5(t)=u(x+h,y,t)$, and $y_6(t)=v(x,y,t)$] are recorded, the initial TF is set as $y_1(t+\Delta t)=\Sigma_{i=1}^{I}c_i\phi_i$ with bases $\phi_i\in\{\Pi_{k=1}^{6}y_k^{d_k}(t)\}$ and $\Sigma_{k=1}^{6}d_k=0,1,2,3$, where $\phi_1=1$ $\phi_2=y_1$, $\phi_3=y_2$, $\phi_4=y_3$, $\phi_5=y_4$, $\phi_6=y_5$, $\phi_7=y_6$, …, $\phi_{49}=y_1y_6^2\ldots\phi_{84}=y_6^3$. This TF has totally 84 terms. As shown in Fig. 3, after the iterative detection procedure is finished, $C(7)$ is the minimum of the $C(r)$ curve and the first seven terms are sequentially 0.016, $0.184y_1$, $0.200y_4$, $-1.000y_1y_6^2$, $0.200y_3$, $0.200y_5$, and $0.200y_2$. Discretizing Eq. (5) with a finite-difference scheme, it has $y_1(t+\Delta t)=F\Delta t+(1-F\Delta t-4D_u\Delta t/h^2)y_1+D_u\Delta t/h^2(y_2+y_4+y_3+y_5)-y_1y_6^2$. Comparing the first seven bases of the final TF with the discretized Gray-Scott model, it can be found that these bases are just the terms of the discretized Eq. (5). In other words, the dynamical structure described by the partial differential Eq. (5) is successfully detected.

The Gray-Scott model has a rich variety of spatiotemporal patterns by making small changes in F and k [1] as shown in

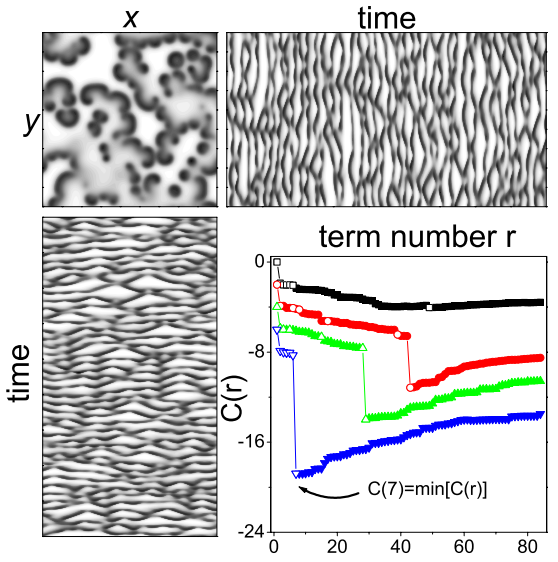

FIG. 3. (Color online). Revealing the simple dynamical structure from complex spatiotemporal pattern governed by partial differential equations (the Gray-Scott model with $F=0.016$ and $K=0.05$). The top left, top right, and bottom left figures illustrate the space $x-y$, time-y, and x time plots, respectively. The bottom right figure plots the information criteria $C(r)$ as a function of term number r, where the definitions of scatters are the same as those in Fig. 2.

Figs. 4(a)–4(d). Applying the proposed scheme to these spatiotemporal signals, the common intrinsic structure $(1, y_1, y_2, y_3, y_4, y_5,$ and $y_1y_6^2)$, especially the high-order term $y_1y_6^2$, governing these patterns can always be detected by the proposed scheme, as shown in Fig. 4(e). On rare occurrences, a few detected terms actually do not belong to the original system (superfluous terms, empty circle scatters in Fig. 4), for example, the terms y_1^2 and $y_5y_6^2$ for $F=0.010$ and the term $y_5y_6^2$ for $F=0.011$. The mistaken detection could be because these terms are highly correlated with some intrinsic terms. This problem can be solved by increasing the number of the data used for the detection. As shown in Fig. 4(f), when the data length is less than 1 000 points, many superfluous terms are wrongly selected, moreover, some intrinsic terms of the original system sometimes could be missed out (square red scatters). When the data length is increased to $1000\sim5000$ points, all intrinsic terms of the original system can always be selected but sometimes a few detected terms are superfluous. When enough points are used for the detection (>5000 points), all intrinsic terms are detected and no superfluous terms are mistakenly involved.

IV. EXPERIMENT

In the last example, we apply the proposed method to experimental data, which was recorded from a Chua's circuit experimental setup [12]. The dynamical behavior of this circuit can be described by the following differential equations:

$$C_1\dot{V}_{C1} = G \times (V_{C1} - V_{C2}) - g(V_{C1}), \tag{7}$$

$$C_2\dot{V}_{C2} = G \times (V_{C1} - V_{C2}) + I_L, \tag{8}$$

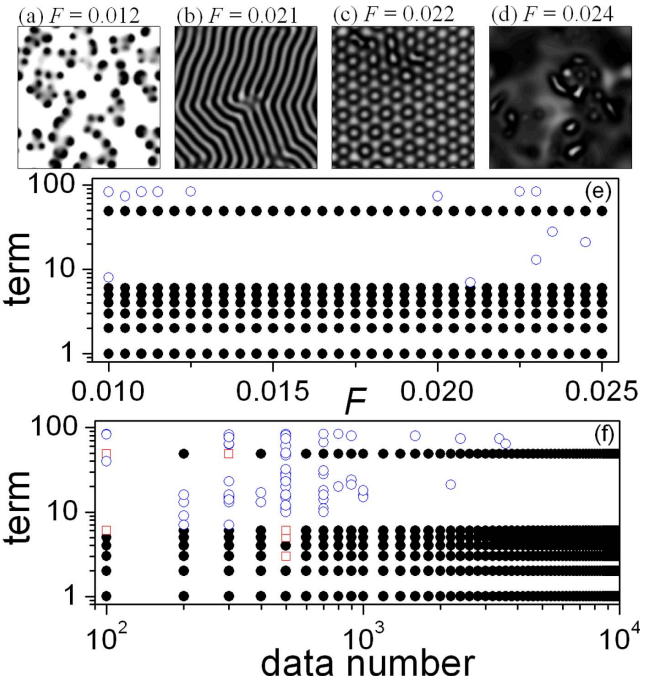

FIG. 4. (Color online). Detection of the common dynamical structure behind various spatiotemporal pattern of the Gray-Scott model controlled by F. (a)–(d) Four typical patterns of the Gray-Scott model with $K=0.05$. (e) Structure detection. (f) The influence of data number. Here, the vertical axis of (e)–(f) represents the index of the basis in the initial TF. When a basis of the initial TF is finally selected by the proposed scheme, a circle scatter will be labeled on its corresponding position. The solid circle black scatters indicate that this detected basis really exists in the original system (intrinsic term), whereas the empty circle blue scatters indicate that the detected basis actually does not belong to the original system (superfluous term). If a basis really belongs to the original system but it is not detected by the proposed scheme (missed term), a square red scatter is labeled on its corresponding position.

$$L\dot{I}_L = -V_{C2} - R_0 I_L, \tag{9}$$

where $g(x)$ is a piecewise-linear function

$$g(x) = \begin{cases} m_1 x + b_1 & (x < B_{p1}) \\ m_{12} x & (B_{p1} \le x \le B_{p2}) \\ m_2 x + b_2 & B_{p2} < x \end{cases}, \tag{10}$$

with $b_1=(m_{12}-m_1)B_{P1}$ and $b_2=(m_{12}-m_1)B_{P2}$. The circuit parameters have been given in Table I. The time series of V_{C1} and V_{C2} of the Chua's circuit were recorded through the oscilloscope (Tektronix TDS-460) with the sampling frequency

TABLE I. Parameter values of Chua circuit.

C_1	5.13	nF	B_{p1}	−1.59	V
C_2	51.1	nF	B_{p2}	1.59	V
G	0.675	mS	m_1	−0.512	mS
L	9.48	mH	m_2	−0.511	mS
R_0	3.46	Ω	m_{12}	−0.835	mS

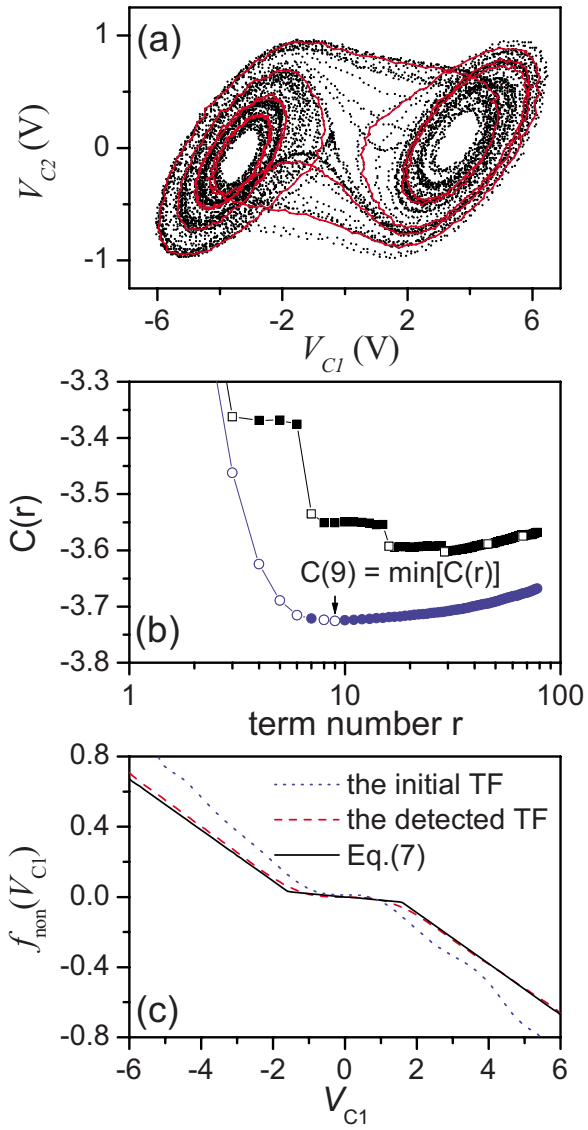

FIG. 5. (Color online). Detection of dynamical structure of a Chua's circuit. (a) the V_{C1} vs V_{C2} phase portrait of the Chua's circuit, where the solid (red) orbits represents the 1,000 points used for the structure detection. (b) The information criteria $C(r)$ of the initial TF (square black scatters), the final TF (circle blue scatters), where the empty scatters represents those intrinsic bases. (c) the detected nonlinear structure of Chua's circuit, where the dashed red line represents the sum of the detected nonlinear terms, the dotted blue line represents the sum of the nonlinear terms of the initial TF, and the solid black line represents the nonlinear component directly deduced from Eq. (7).

0.5 MHz (the sampling interval $\Delta t=2$ μs). Figure 5(a) presents the V_{C1} vs V_{C2} phase portrait of the experimentally measured circuit system. In this system, the function $g(x)$ in Eq. (7) is nonlinear, which causes the chaotic behavior of the Chua's circuit.

Although 10 000 points were recorded in our experiments [the solid dots in Fig. 5(a)], only a short phase orbit with 1 000 points is used for the structure detection [the solid red line in Fig. 5(a)]. The fluctuations in the orbits are due to the noise in the practical circuit system. A TF with numerous bases $V_{C1}(t+\Delta t)=\Sigma_{i=1}^{I}c_i\phi_i$, where $\phi_i \in \{V_{C1}^{d_1}(t)\times V_{C2}^{d_2}(t)\}$ with $d_1+d_2=0,1,\ldots 11$, is used to approach the original system. In this TF, there are a total of 78 bases. After the iterative detection procedure is finished, $C(9)$ is the minimum of the $C(r)$ curve and the first nine terms are sequentially $\phi_1=1$, $\phi_2=V_{C1}$, $\phi_3=V_{C2}$, $\phi_7=V_{C1}^3$, $\phi_{16}=V_{C1}^5$, $\phi_{29}=V_{C1}^7$, $\phi_4=V_{C1}^2$, $\phi_{67}=V_{C1}^{11}$, and $\phi_{46}=V_{C1}^9$ as shown in Fig. 5(b)

Observing Eq. (7), it can be found that Eq. (7) explicitly has the terms V_{C1} and V_{C2}. Moreover, for $m_1\approx m_2$ and $B_{p1}\approx B_{p2}$, The piecewise-linear function $g(x)$ is an odd function [see Eq. (10)], which can be approached by the polynomial $c_1x+c_3x^3+c_5x^5+\cdots+c_{2i-1}x^{(2i-1)}+\ldots$ $(i=1,2,3,\ldots)$. In other words, the terms $V_{C1}^{d_1}$ with odd powers are the intrinsic terms of the Chua's circuit [Eq. (7)], but the terms $V_{C1}^{d_1}$ with even powers are superfluous terms. Therefore, the proposed scheme has successfully detected all intrinsic terms (V_{C1}, V_{C2}, V_{C1}^3, V_{C1}^5, V_{C1}^7, V_{C1}^9, and V_{C1}^{11}) and excluded numerous superfluous terms. In addition, the term V_{C1}^2 and the constant term detected by the proposed scheme might be ascribed to the noise effects in the practical circuit system.

Using the detected basis, the nonlinear structure of Chua's circuit can be well approached, as shown in Fig. 5(c). The sum of the nonlinear terms

$$[f_{\text{non}}(V_{C1}) = -1.854\times10^{-3} - 1.811\times10^{-2}V_{C1}^3 + 1.449\times10^{-3}V_{C1}^5 - 6.254\times10^{-5}V_{C1}^7 + 6.624\times10^{-4}V_{C1}^2 - 1.170\times10^{-8}V_{C1}^{11} + 1.360\times10^{-6}V_{C1}^9]$$

detected by the proposed method is plotted in this figure with a dashed red line. The sum of the nonlinear terms

$$[f_{\text{non}}(V_{C1}) = c_1 + c_3V_{C1}^0V_{C2}^1 + c_4V_{C1}^2V_{C2}^0 + c_5V_{C1}^1V_{C2}^1 + \cdots + c_{78}V_{C1}^0V_{C2}^{11}$$

with $V_{C2}=0$] of the initial TF is also plotted in the same figure with a dotted blue line. In this figure, the linear term c_2V_{C1} is eliminated. This is because the linear term is so large that it could make the nonlinear characteristics invisible. For the sake of comparison, the nonlinear component $f_{\text{non}}(V_{C1})=f(V_{C1})-1.608V_{C1}$ directly deduced from Eq. (7) is also plotted in Fig. 5(c) with a solid black line, where $f(V_{C1})=(1+G\Delta t/C_1)V_{C1}-g(V_{C1})$ is obtained by discretizing Eq. (7) with a finite-difference scheme. The term $1.608V_{C1}$ is the linear term of the polynomial $c_1+c_2V_{C1}+c_2V_{C1}^2+c_3V_{C1}^3+\ldots$, which can best fit the function $f(V_{C1})=(1+G\Delta t/C_1)V_{C1}-g(V_{C1})$. It can be seen that the final TF can approach the real Chua's circuit system very well.

In a previous study, the structure selection method based on error reduction ratio was also applied to Chua's system [20]. It was found that the accurate estimation of polynomial models from the noise data is very difficult [20]. In this study, the successful application to experimental data with noise shows the advantage of the proposed method. In addition, the dynamical structure of the Chua's circuit is not polynomial nature, but a precise-linear function. The polynomial detected by the proposed method can still closely ap-

proach its structure. These results could validate the performance of the proposed method under a complex and realistic situation.

V. CONCLUSION

In summary, a scheme is proposed to detect the global structures (mathematic equations) of nonlinear systems from chaotic series. The successful detections of the logistic map and Gray-Scott model validate the proposed scheme. Especially, numerical simulations show that this method is robust to the data length and noise. This advantage could broaden the application of the proposed scheme to realistic systems. Finally, the proposed scheme is utilized to detect the dynamical structure of a Chua's circuit, which confirms its capacity for real systems.

The polynomial is one kind of typical nonlinear structure, which frequently exists in the dynamical structure of the nonlinear system. Moreover, the other kinds of functions can be approximated by the polynomial. If it is not known what kinds of terms exist in the original system, the polynomial can be used to approximate the nonlinear structure in these systems. As we have done in the study of Chua's circuit, the nonlinear structure described by the piecewise-linear function $g(x)$ is approximated by the polynomial. Therefore, we chose the TFs only containing polynomial terms in this study. If the TFs consist of other bases, the validation of the proposed method will be examined in the future works.

ACKNOWLEDGMENT

This work was supported by NSF of China under Grants No. 10904069 and No. 10874088.

[1] J. E. Pearson, Science **261**, 189 (1993).
[2] R. Hegger, M. J. Bünner, H. Kantz, and A. Giaquinta, Phys. Rev. Lett. **81**, 558 (1998).
[3] B. P. Bezruchko, A. S. Karavaev, V. I. Ponomarenko, and M. D. Prokhorov, Phys. Rev. E **64**, 056216 (2001).
[4] D. Ghosh and S. Banerjee, Phys. Rev. E **78**, 056211 (2008).
[5] L. A. Aguirre, E. C. Furtado, and L. A. B. Torres, Phys. Rev. E **74**, 066203 (2006).
[6] H. Voss and J. Kurths, Phys. Lett. A **234**, 336 (1997).
[7] C. Tao, Y. Zhang, G. Du, and J. J. Jiang, Phys. Lett. A **332**, 197 (2004).
[8] G. Gouesbet and C. Letellier, Phys. Rev. E **49**, 4955 (1994).
[9] B. P. Bezruchko and D. A. Smirnov, Phys. Rev. E **63**, 016207 (2000).
[10] L. A. Aguirre and E. C. Furtado, Phys. Rev. E **76**, 046219 (2007).
[11] C. Tao, Y. Zhang, G. Du, and J. J. Jiang, Phys. Rev. E **69**, 036204 (2004).
[12] C. Tao, Y. Zhang, and J. J. Jiang, Phys. Rev. E **76**, 016209 (2007).
[13] R. Hegger, A. Altis, P. H. Nguyen, and G. Stock, Phys. Rev. Lett. **98**, 028102 (2007).
[14] L. A. Aguirre, U. S. Freitas, C. Letellier, and J. Maquet, Physica D **158**, 1 (2001).
[15] J. B. Kadtke, J. Brush, and J. Holzfuss, Int. J. Bifurcation Chaos Appl. Sci. Eng. **3**, 607 (1993).
[16] J. P. Crutchfield and B. S. McNamara, Complex Syst. **1**, 417 (1987).
[17] K. Judd and A. Mees, Physica D **82**, 426 (1995).
[18] M. Small and C. K. Tse, Phys. Rev. E **66**, 066701 (2002).
[19] G. Kerschen, B. F. Feeny, and J.-C. Golinval, Comput. Methods Appl. Mech. Eng. **192**, 1785 (2003).
[20] L. A. Aguirre and S. A. Billings, Physica D **85**, 239 (1995).
[21] M. Abel, K. Ahnert, J. Kurths, and S. Mandelj, Phys. Rev. E **71**, 015203(R) (2005).
[22] Y. I. Molkov, D. N. Mukhin, E. M. Loskutov, A. M. Feigin, and G. A. Fidelin, Phys. Rev. E **80**, 046207 (2009).
[23] K. M. Short and A. T. Parker, Phys. Rev. E **58**, 1159 (1998).
[24] M. Barahona and C.-S. Poon, Nature (London) **381**, 215 (1996).
[25] C.-S. Poon and C. K. Merrill, Nature (London) **389**, 492 (1997).
[26] C.-S. Poon and M. Barahona, Proc. Natl. Acad. Sci. U.S.A. **98**, 7107 (2001).
[27] F. Takens, *Lecture Notes in Mathematics* (Springer, Berlin, 1980), Vol. 898, p. 366.
[28] P. Gray and S. K. Scott, Chem. Eng. Sci. **39**, 1087 (1984).
[29] H. Wang and Q. Ouyang, Phys. Rev. Lett. **99**, 214102 (2007).